

Supporting Information

Thermal-facilitated interfacial polymerization toward high-performance polyester desalination membrane

Jianliang Shen,^{ab} Guangzhe Wang,^{ab} Xinda You,^{ab} Benbing Shi,^{ab} Jing Xue,^{ab} Jingqiu Yuan,^{ab} Yafei Li,^{ab} Jingyuan Guan,^{ab} Yu Ma,^{ab} Yanlei Su,^{ab} Runnan Zhang*^{ab} and Zhongyi Jiang*^{abc}

^a *Key Laboratory for Green Chemical Technology, School of Chemical Engineering and Technology, Tianjin University, Tianjin 300072, China*

^b *Collaborative Innovation Center of Chemical Science and Engineering (Tianjin), Tianjin, 300072, China*

^c *Joint School of National University of Singapore and Tianjin University, International Campus of Tianjin University, Binhai New City Fuzhou, 350207, China.*

* *E-mail: runnan.zhang@tju.edu.cn Tel: 86-22-23500086, Fax: 86-22-23500086*

* *E-mail: zhyjiang@tju.edu.cn Tel: 86-22-23500086, Fax: 86-22-23500086*

1. Experimental

1.1 Polyester membrane preparation

To further investigate the influence of elevated temperature on the polyester network structure and the separation performance, Glu-TMC(30), Glu-TMC(40) and Glu-TMC(60) membranes were also prepared. PAN supports were immersed in ethanol for at least 12 h to remove glycerol and other substances and thoroughly washed with DI water. The polyester membrane was prepared on PAN support by interfacial polymerization as follows. Firstly, PAN support was soaked into 2.0 wt% glucose aqueous solution for 2 min. The pH of the aqueous solution was adjusted to 13.0 by sodium hydroxide. Then a filter paper was employed to remove excess aqueous solution on top surface of glucose loaded support. Subsequently, the glucose loaded support was gently dipped into n-heptane solution containing 0.2 wt% TMC to process IP for 10 min at the temperature of 30, 40 or 60°C. The as-prepared membrane was then dried in an oven at 60°C for 20 min for further crosslinking. Finally, the resultant polyester thin film composite (PE-TFC) membranes, denoted as Glu-TMC(x), where x stands for the reaction temperature, were rinsed and stored in DI water for further use. Sucrose, Raffinose and β -CD were also used to prepare PE-TFC membranes and the fabrication procedure was the same as mentioned above, and the resultant membranes were denoted as Suc-TMC(x), Raf-TMC(x) and β -CD-TMC(x), respectively.

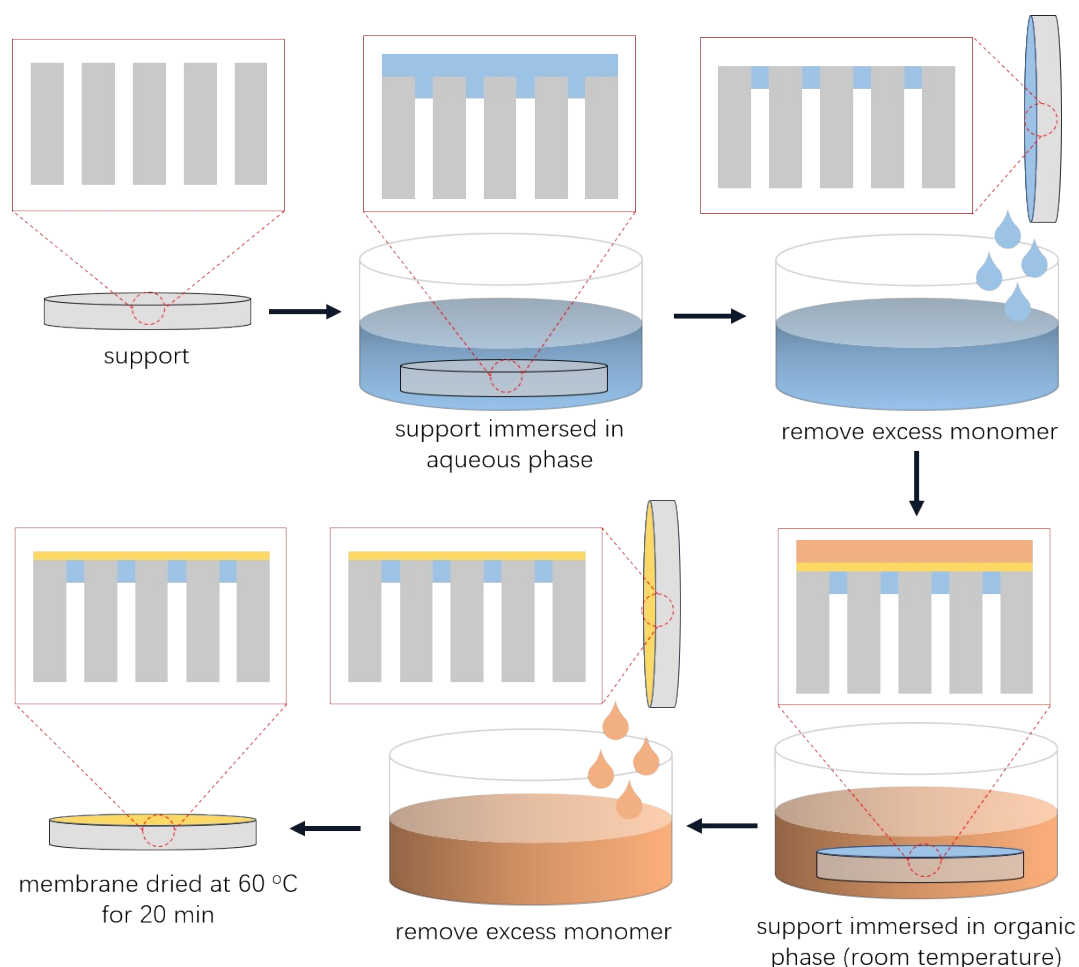


Fig. S1 Schematic diagram of the conventional IP process. Conventional IP was performed at 20°C.

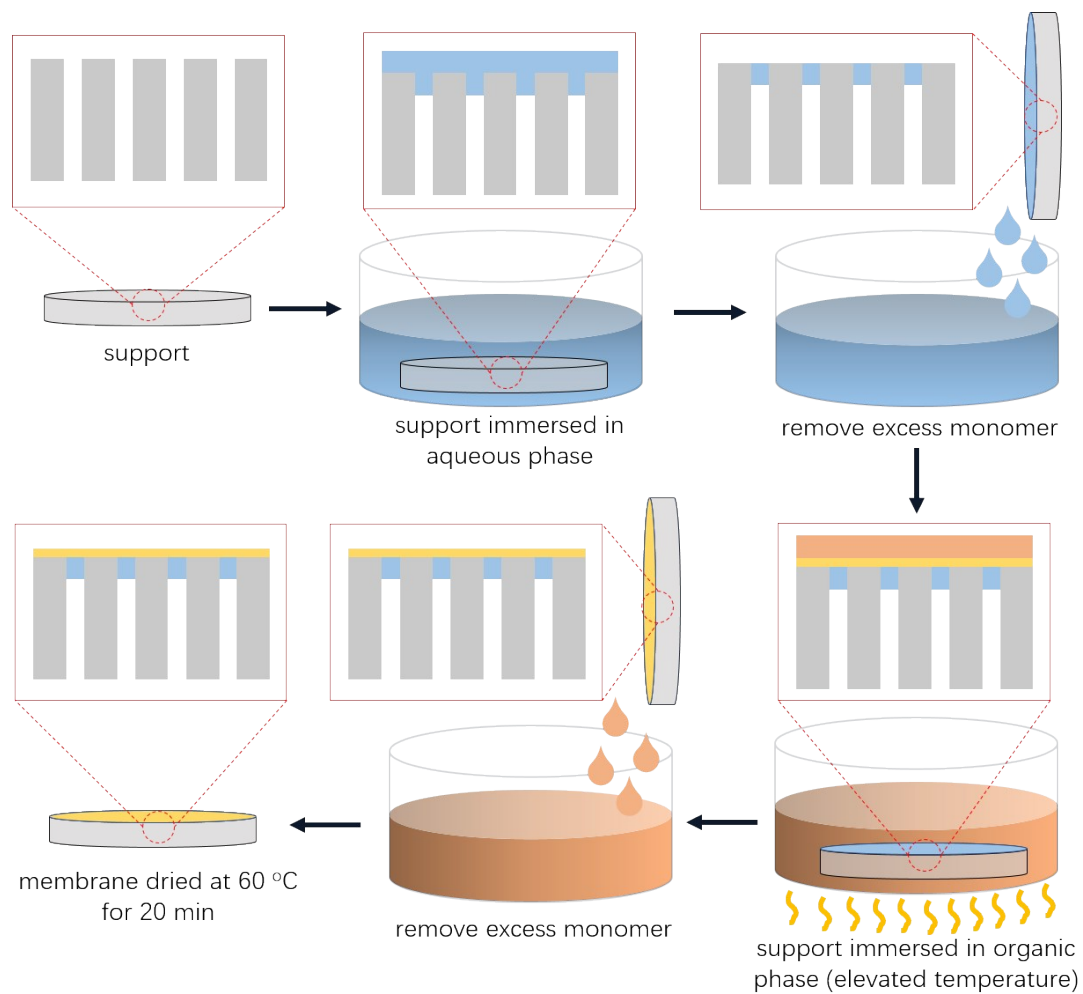


Fig. S2 Schematic diagram of the TFIP process. TFIP was performed at 50°C.

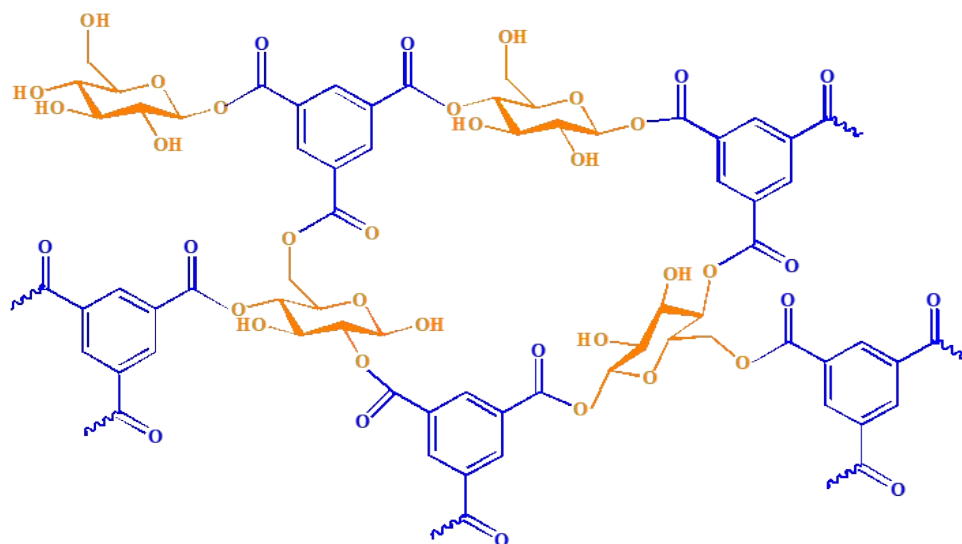


Fig. S3 The probable reaction routes between glucose and TMC.

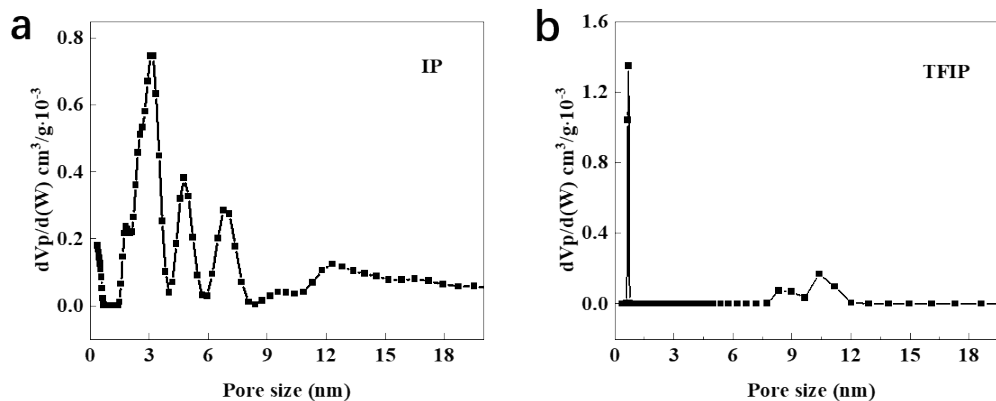


Fig. S4 Pore width distribution of PE-TFC membranes formed via (a) IP and (b) TFIP analyzed by BET N_2 adsorption isotherm using DFT model.

To verify the reaction between glucose and TMC performed at oil/water interfacial zone, FTIR-ATR analysis of the membranes was conducted. As shown in Fig. S5, the peak at 1728 cm^{-1} attributed to $C=O$ was observed for both PAN support and the polyester TFC membranes. This can be explained that the cyano group is partially hydrolyzed to carboxyl group. However, the peak at 1728 cm^{-1} of polyester membranes was stronger than that of PAN support, indicating the successful reaction between hydroxyl groups in glucose and acyl chloride groups in TMC. New peaks at 1239 cm^{-1} are characteristic of $C-O-C$, while broad characteristic peaks located in $3200\text{-}3700\text{ cm}^{-1}$ may be ascribed to the residual unreacted hydroxyl groups. The results above verified the successful formation of a polyester film.

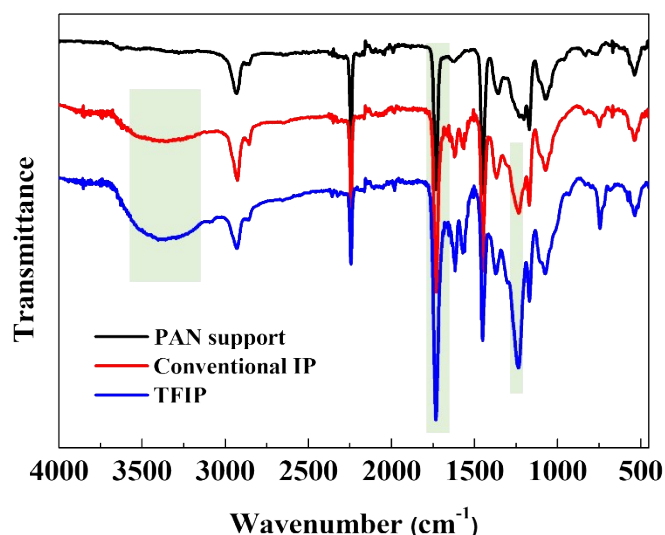


Fig. S5 FTIR-ATR spectrum of the Glu-TMC(20) and Glu-TMC(50) membranes formed via conventional IP and TFIP, respectively.

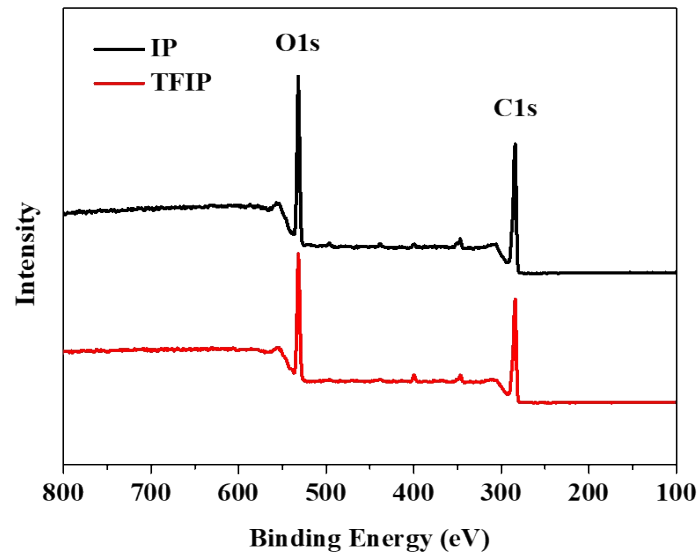


Fig. S6 XPS spectra of Glu-TMC(20) and Glu-TMC(50) membranes fabricated from IP and TFIP, respectively.

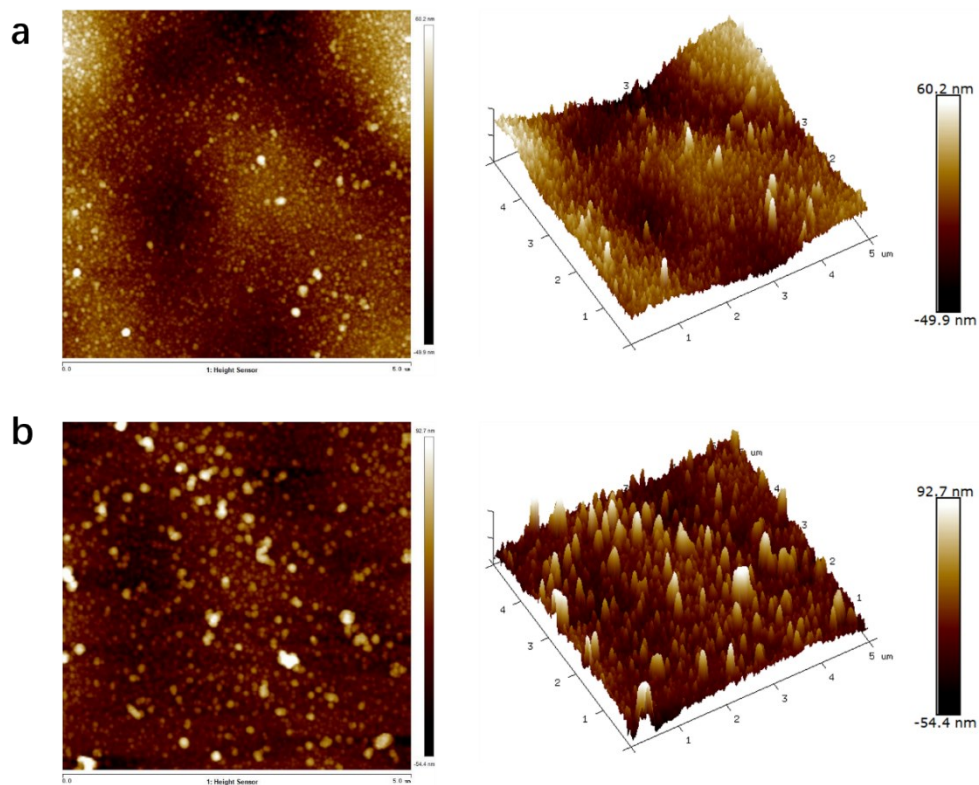


Fig. S7 AFM topography of (a) Glu-TMC(20) membrane formed via conventional IP and (b) Glu-TMC(50) membrane formed via TFIP with scanning area of 5 μm by 5 μm, respectively.

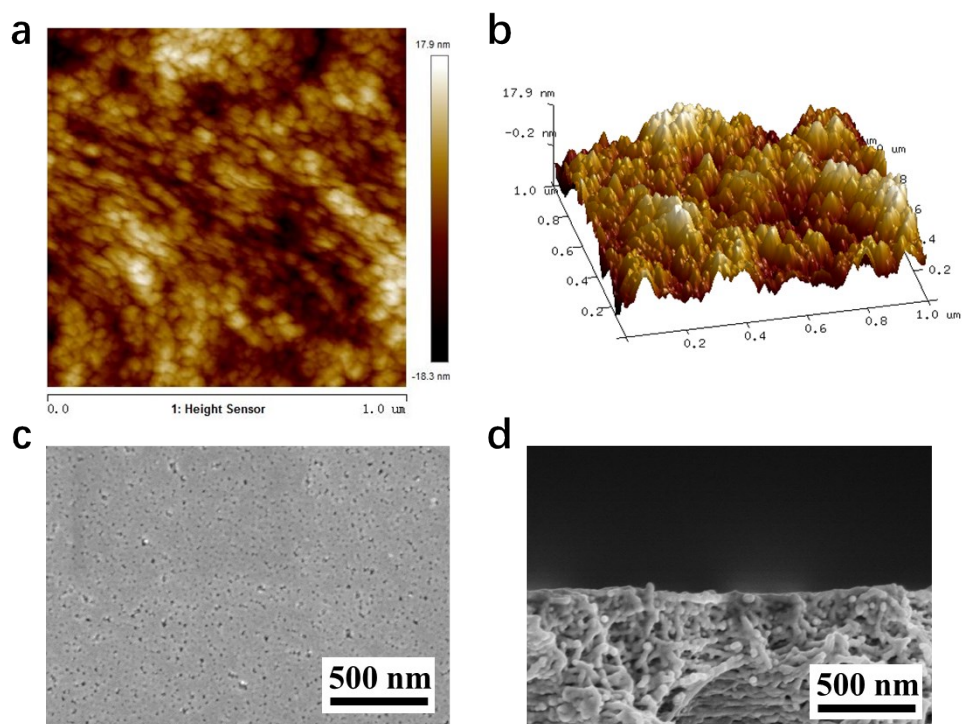


Fig. S8 (a) and (b) AFM topography of top surface of PAN support with scanning area of $1\ \mu\text{m}$ by $1\ \mu\text{m}$. SEM images of the (c) top surface and (d) cross section of PAN support.

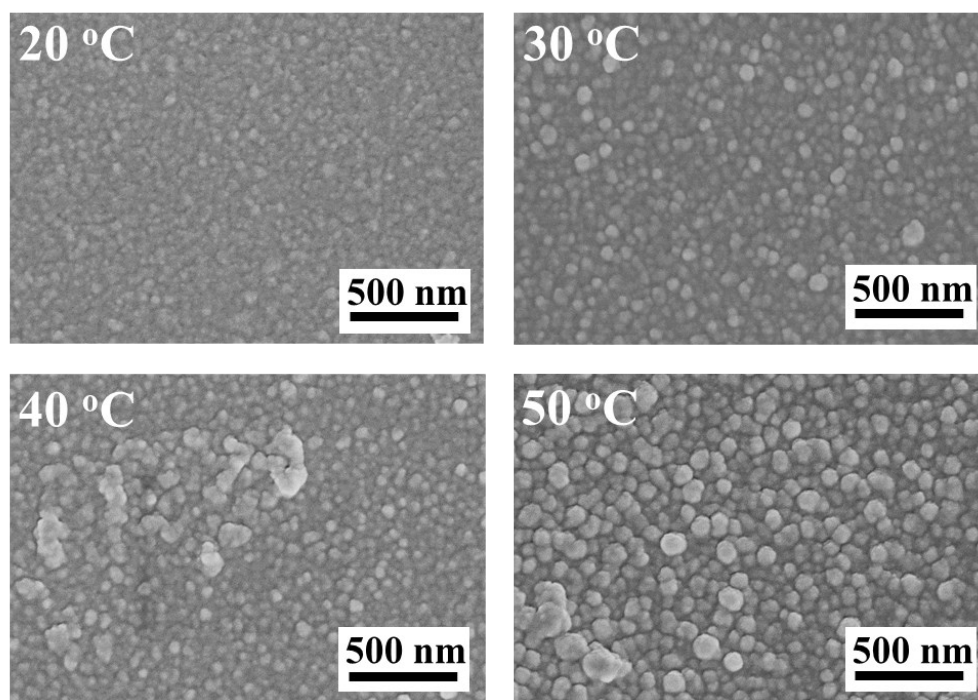


Fig. S9 Morphologies of top surface of Glu-TMC membranes. The temperature in the upper left corner of the image represents the reaction temperature of IP process.

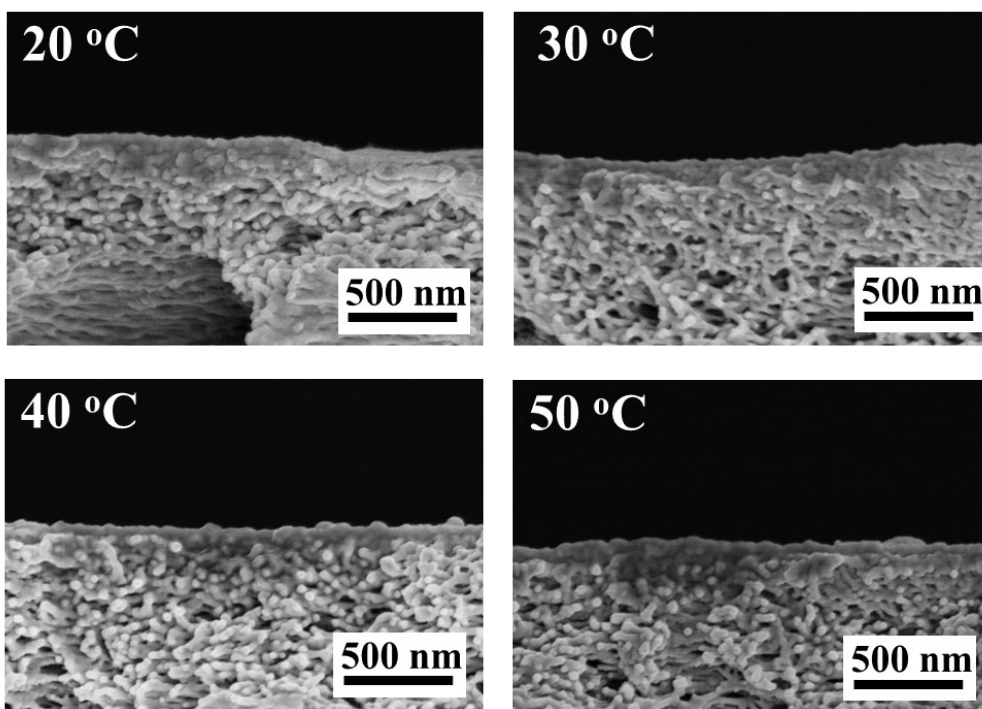


Fig. S10 Morphologies of cross section of Glu-TMC membranes. The temperature in the upper left corner of the image represents the reaction temperature of IP process.

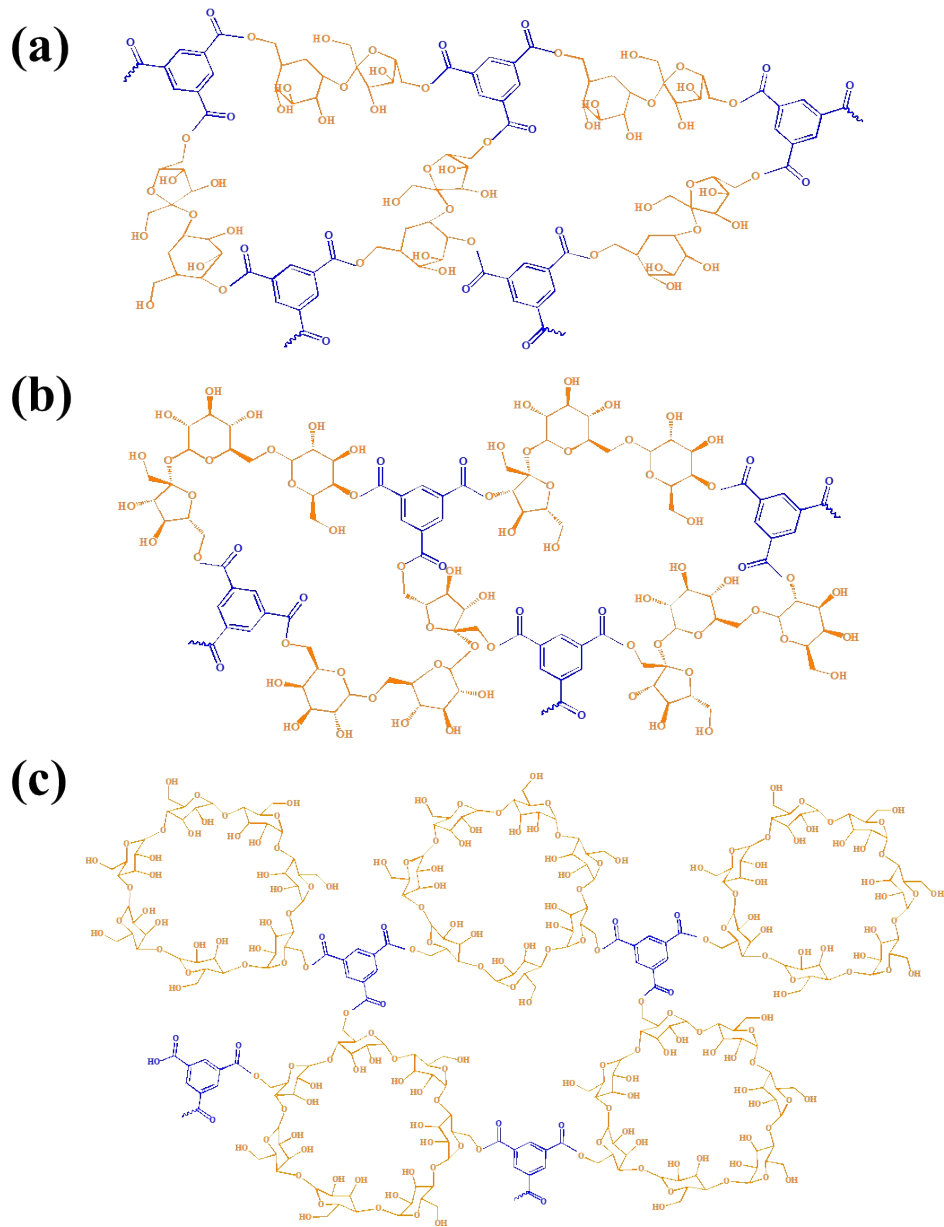


Fig. S11 The probable reaction routes between (a) sucrose, (b) raffinose and (c) β -CD with TMC.

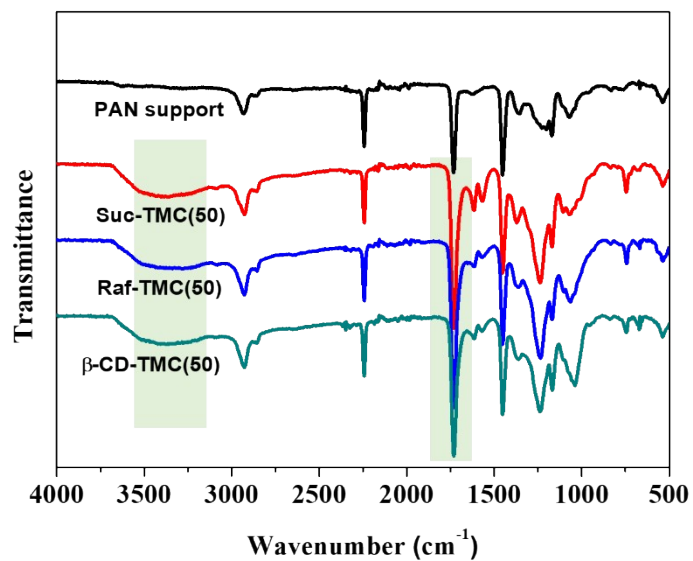


Fig. S12 FTIR-ATR spectrum of PAN support, Suc-TMC(50), Raf-TMC(50) and β -CD-TMC(50) membranes.

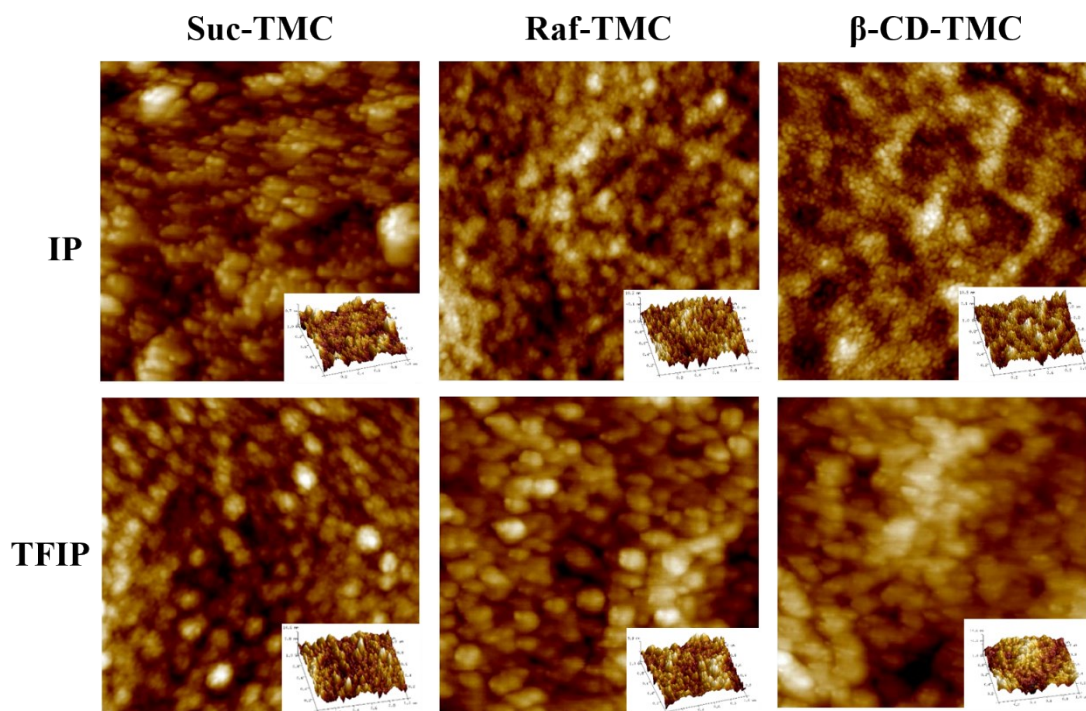


Fig. S13 AFM topography of Suc-TMC, Raf-TMC and β -CD-TMC membranes formed via conventional IP (20°C) and TFIP (50°C). Scanning area of 1 μm by 1 μm .

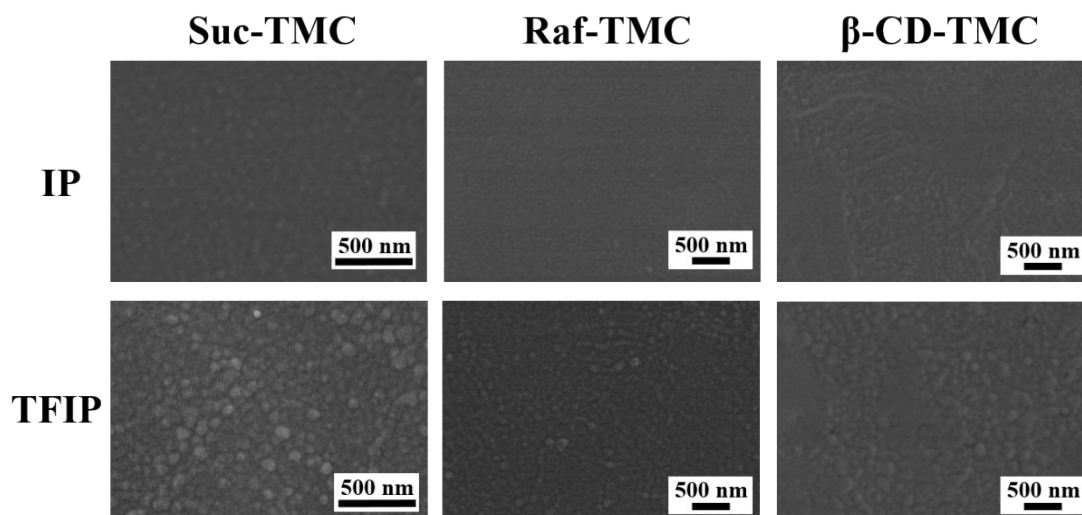


Fig. S14 Morphologies of top surface of Suc-TMC, Raf-TMC and β -CD-TMC membranes formed via conventional IP (20°C) and TFIP (50°C).

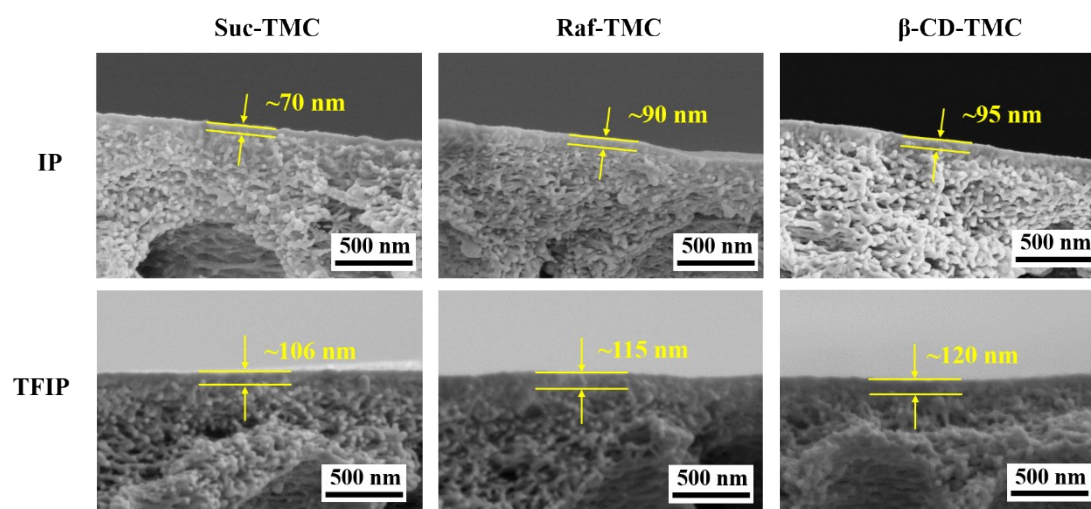


Fig. S15 Cross-section SEM images of the PE-TFC membranes prepared via conventional IP and TFIP, respectively.

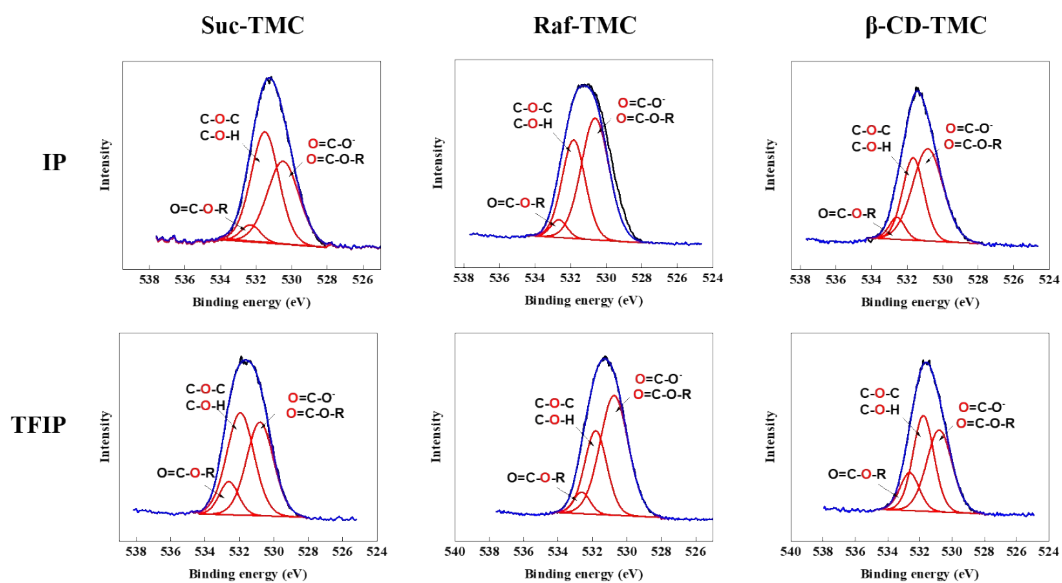


Fig. S16 XPS spectra of the polyester active layer from PE-TFC membranes formed via conventional IP and TFIP, respectively.

Table S1. Surface area increase of the saccharide-based membranes formed by TFIP.

Sample	Surface area increase (%)
Glu-TMC(50)	15.4±2.0
Suc-TMC(50)	4.3±1.4
Raf-TMC(50)	5.5±1.9
β-CD-TMC(50)	3.6±1.1

Table S2. Cross-linking density of the polyester membranes.

Sample	Cross-linking density (%)
Glu-TMC(20)	7.1
Glu-TMC(50)	30.2
Suc-TMC(20)	12.1
Suc-TMC(50)	22.9
Raf-TMC(20)	8.3
Raf-TMC(50)	10.5
β-CD-TMC(20)	12.2
β-CD-TMC(50)	34.4

Table S3 Performance comparison of various membranes towards salt ion rejection.

Polyester membranes	Permeance (L·m ⁻² ·h ⁻¹ ·bar ⁻¹)	Na ₂ SO ₄ rejection (%)	Operation pressure (MPa)	Ref.
PE-TMC/PES	1.2	98.1	0.5	1
TEOA-TMC/PSf	2.5	82.2	0.6	2
TA-TMC/PES	24.4	49.0	0.2	3
HPE-TMC/PAN	8.5	91.0	0.2	4
TA/GOQDs	11.6	57.1	0.2	5
Res/Phg	7.4	92.5	0.5	6
β-CD/TEOA-TMC	2.3	82.0	0.6	7
TiO ₂ -PAR	20.5	21.7	0.2	8
Commercial NF (e.g. DK, DL)	5-14	40-98	6-15	9
Glu-TMC(50)	16.1	99.5	0.3	This work
Suc-TMC(50)	7.7	97.4	0.3	
Raf-TMC(50)	8.2	88.5	0.3	
β-CD-TMC(50)	7.6	94.6	0.3	

References

- [1] J. Cheng, W. Shi, L. Zhang and R. Zhang, *Appl. Surf. Sci.*, 2017, 416, 152-159.
- [2] B. Tang, Z. Huo and P. Wu, *J. Membr. Sci.*, 2008, 320, 198-205.
- [3] Y. Zhang, Y. Su, J. Peng, X. Zhao, J. Liu, J. Zhao and Z. Jiang, *J. Membr. Sci.*, 2013, 429, 235-242.
- [4] X. Wei, X. Kong, J. Yang, G. Zhang, J. Chen and J. Wang, *J. Membr. Sci.*, 2013, 440, 67-76.
- [5] C. Zhang, K. Wei, W. Zhang, Y. Bai, Y. Sun and J. Gu, *ACS Appl. Mater. Interfaces*, 2017, 9(12): 11082-11094.
- [6] A. Bera, D.V. Bhalani, S.K. Jewrajka and P.K. Ghosh, *RSC Adv.*, 2016, 6, 99867-99877.
- [7] H. Wu, B. Tang and P. Wu, *J. Membr. Sci.*, 2013, 428, 301-308.
- [8] R. Zhang, Y. Liu, M. He, M. Wu, Z. Jiao, Y. Su, Z. Jiang, P. Zhang and X. Cao, *J. Membr. Sci.*, 2018, 555, 337-347.
- [9] M. Zhang, K. Guan, Y. Ji, G. Liu, W. Jin and N. Xu, *Nat. Commun.*, 2019, 10, 1253.